EUR 516.e
REPRINT

EUROPEAN ATOMIC ENERGY COMMUNITY - EURATOM

CARBON TRANSPORT

by

L.J. VALETTE

1964

DRAGON PROJECT

Reprinted from
DE INGENIEUR
Vol. 75, No. 11 - 1963

LEGAL NOTICE

This document was prepared under the sponsorship of the Commission of the European Atomic Energy Community (EURATOM).

Neither the EURATOM Commission, its contractors nor any person acting on their behalf :

1° — Make any warranty or representation, express or implied, with respect to the accuracy, completeness, or usefulness of the information contained in this document, or that the use of any information, apparatus, method, or process disclosed in this document may not infringe privately owned rights; or

2° — Assume any liability with respect to the use of, or for damages resulting from the use of any information, apparatus, method or process disclosed in this document.

EUR 516.e

REPRINT

CARBON TRANSPORT by L.J. VALETTE.

European Atomic Energy Community - EURATOM.
DRAGON PROJECT.
Reprinted from "DE INGENIEUR" - Vol. 75, No. 11 - 1963 - pp. 39-49.

The problem of Carbon Transport is defined as the combined removal of graphite from the hot core of the reactor and the back deposition of carbon on metallic components at lower temperature. This Carbon Transport is the result of temperature reversible reactions which occur between reactor materials and the impurities present in the coolant helium.

A brief survey is made of the important variables affecting the Carbon Transport process; which are oxidation, carbon deposition, purification, in-leakage, and outgassing of gaseous impurities.

Based on the information available in literature it is shown that the extend of oxidation of graphite is governed by three single processes, the chemical reaction rate, the diffusion of the impurities in the graphite pores, and diffusion

EUR 516.e

REPRINT

CARBON TRANSPORT by L.J. VALETTE.

European Atomic Energy Community - EURATOM.
DRAGON PROJECT.
Reprinted from "DE INGENIEUR" - Vol. 75, No. 11 - 1963 - pp. 39-49.

The problem of Carbon Transport is defined as the combined removal of graphite from the hot core of the reactor and the back deposition of carbon on metallic components at lower temperature. This Carbon Transport is the result of temperature reversible reactions which occur between reactor materials and the impurities present in the coolant helium.

A brief survey is made of the important variables affecting the Carbon Transport process; which are oxidation, carbon deposition, purification, in-leakage, and outgassing of gaseous impurities.

Based on the information available in literature it is shown that the extend of oxidation of graphite is governed by three single processes, the chemical reaction rate, the diffusion of the impurities in the graphite pores, and diffusion

EUR 516.e

REPRINT

CARBON TRANSPORT by L.J. VALETTE.

European Atomic Energy Community - EURATOM.
DRAGON PROJECT.
Reprinted from "DE INGENIEUR" - Vol. 75, No. 11 - 1963 - pp. 39-49.

The problem of Carbon Transport is defined as the combined removal of graphite from the hot core of the reactor and the back deposition of carbon on metallic components at lower temperature. This Carbon Transport is the result of temperature reversible reactions which occur between reactor materials and the impurities present in the coolant helium.

A brief survey is made of the important variables affecting the Carbon Transport process; which are oxidation, carbon deposition, purification, in-leakage, and outgassing of gaseous impurities.

Based on the information available in literature it is shown that the extend of oxidation of graphite is governed by three single processes, the chemical reaction rate, the diffusion of the impurities in the graphite pores, and diffusion

of the impurities from the main coolant to the graphite surface. Each of these processes becomes preponderant in different temperature ranges.

In the second part of the paper some aspects of the corrosion of Dragon fuel element components are discussed. Due to the temperature dependence of the reaction it is shown that corrosion along the fuel rod will be unevenly distributed and due to the high coolant flow, the depletion of impurities along these rods is negligible. On the other hand, in the purge channel the rate of depletion of impurities is very much more pronounced, due to the small flow and the high graphite temperature. The calculations show that the top fuel boxes will be very severely damaged on a short distance.

Finally, in order to prevent this last danger it is proposed to insert a get er for the impurities in the inlet purge flow.

of the impurities from the main coolant to the graphite surface. Each of these processes becomes preponderant in different temperature ranges.

In the second part of the paper some aspects of the corrosion of Dragon fuel element components are discussed. Due to the temperature dependence of the reaction it is shown that corrosion along the fuel rod will be unevenly distributed and due to the high coolant flow, the depletion of impurities along these rods is negligible. On the other hand, in the purge channel the rate of depletion of impurities is very much more pronounced, due to the small flow and the high graphite temperature. The calculations show that the top fuel boxes will be very severely damaged on a short distance.

Finally, in order to prevent this last danger it is proposed to insert a getter for the impurities in the inlet purge flow.

of the impurities from the main coolant to the graphite surface. Each of these processes becomes preponderant in different temperature ranges.

In the second part of the paper some aspects of the corrosion of Dragon fuel element components are discussed. Due to the temperature dependence of the reaction it is shown that corrosion along the fuel rod will be unevenly distributed and due to the high coolant flow, the depletion of impurities along these rods is negligible. On the other hand, in the purge channel the rate of depletion of impurities is very much more pronounced, due to the small flow and the high graphite temperature. The calculations show that the top fuel boxes will be very severely damaged on a short distance.

Finally, in order to prevent this last danger it is proposed to insert a getter for the impurities in the inlet purge flow.

The Dragon Project [1])

621.039.524.2

VI. Carbon Transport

by L. J. Valette, (Belgium). Research & Development Division, Dragon Project. Chemistry Branch.
Group Leader of the section Mass Transfer Studies

Summary: The problem of Carbon Transport is defined as the combined removal of graphite from the hot core of the reactor and the back deposition of carbon on metallic components at lower temperature. This Carbon Transport is the result of temperature reversible reactions which occur between reactor materials and the impurities present in the coolant helium.

A brief survey is made of the important variables affecting the Carbon Transport process; which are oxidation, carbon deposition, purification, in-leakage, and outgassing of gaseous impurities.

Based on the information available in literature it is shown that the extend of oxidation of graphite is governed by three single processes, the chemical reaction rate, the diffusion of the impurities in the graphite pores, and diffusion of the impurities from the main coolant to the graphite surface. Each of these processes becomes preponderant in different temperature ranges.

In the second part of the paper some aspects of the corrosion of Dragon fuel element components are discussed. Due to the temperature dependence of the reaction it is shown that corrosion along the fuel rod will be unevenly distributed and due to the high coolant flow, the depletion of impurities along these rods is negligible. On the other hand, in the purge channel the rate of depletion of impurities is very much more pronounced, due to the small flow and the high graphite temperature. The calculations show that the top fuel boxes will be very severely damaged on a short distance.

Finally, in order to prevent this last danger it is proposed to insert a getter for the impurities in the inlet purge flow.

1. Introduction

In the Dragon Reactor, Carbon Transport may result from the combined effect of corrosion of high temperature graphite in the core and back deposition of the carbon on metallic surfaces at a lower temperature. Transport of carbon may thus occur by reversible temperature dependent reactions with gaseous impurities such as O_2, H_2, CO_2 and CO present in the circuit at the vpm levels.

The thermodynamically possible reactions at Dragon operating temperatures are listed below:- [1]

$$C + O_2 \longrightarrow CO_2 \quad (1)$$

$$2C + O_2 \longrightarrow 2CO \quad (2)$$

$$C + CO_2 \rightleftharpoons 2CO \quad (3)$$

$$C + H_2O \rightleftharpoons CO + H_2 \quad (4)$$

$$C + 2H_2 \rightleftharpoons CH_4 \quad (5)$$

$$2C + 2H_2O \rightleftharpoons CH_4 + CO_2 \quad (6)$$

$$2C + N_2 + H_2 \rightleftharpoons 2HCN \quad (7)$$

$$CO + 3H_2 \rightleftharpoons CH_4 + H_2O \quad (8)$$

$$CO + H_2O \rightleftharpoons CO_2 + H_2 \quad (9)$$

We consider here mainly the kinetic region of the reactions, because, although thermodynamically possible, the reactions must start at a sufficiently high rate for the carbon transport process to be significant.

The final objective of the research programme is to specify the impurity level admissible.

2. Variables affecting Carbon Transport in a Reactor System

To be of any importance in an H.T.G.C.R. the chemical reactions must as already stated, start at a significant speed. The

[1]) Voordrachten gehouden voor de Afdeling voor Kerntechniek van het K. I. v. I., in samenwerking met het Reactor Centrum Nederland en het Ned. Atoomforum, op 6 april 1962 te 's Gravenhage. Zie *De Ingenieur* 1962 Nr. 12 blz. A 180.

speed of reaction is dependent on the level of impurity and the nature of impurity in the system.

The level of impurities will depend on their rates of purification and in-leakage. The equilibrium ratio between the graphite oxidising impurities and their by-products will depend on the rate of *combustion of graphite* and the rate of regeneration of the oxidant by *carbon deposition*, respectively.

2.1 *Oxidation of Graphite*

Extensive work has been so far done on the oxidation of graphite and carbon. Although the results are not directly applicable to a reactor system, is has been clearly established that the heterogeneous reaction with a porous graphite may be controlled by three main processes: fig. 1.

The chemical reaction rate

In-pore Diffusion in the pores giving access to the internal reacting surfaces.

Diffusion in the gaseous boundary layer surrounding the graphite.

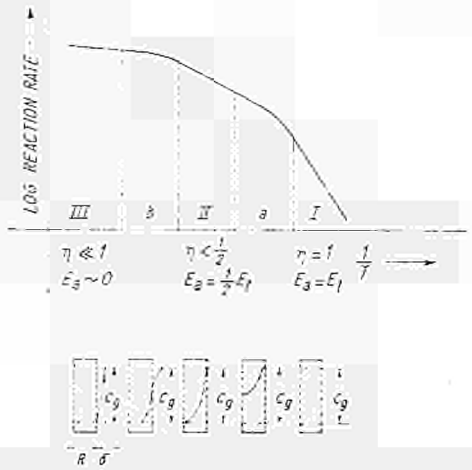

Fig. 1. The three zones of the reaction rate in a porous graphite v.s. temperature.

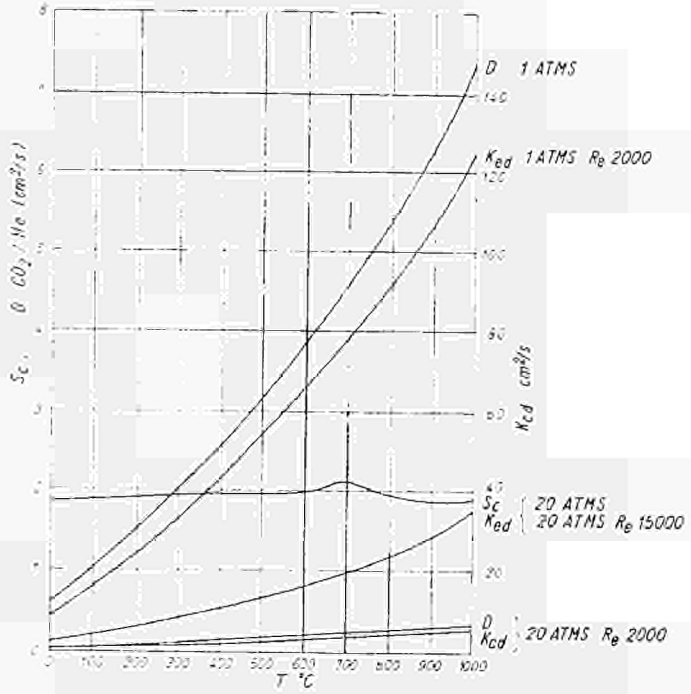

Fig. 2. Mass transfer coefficient K_{cd}, Schmidt No. Sc and diffusivity of CO_2 in He against temperature.

Figure 1 represents the three zones of the porous carbon reaction rate versus temperature [2].

In a reactor system, in addition to these three processes, it is necessary to consider the enhancement of the reactions by:-

The in-pile radiation effect on graphite

2.1.1 *Chemical reaction rate*

At the lower temperature, when the whole internal surface of the graphite is accessible to the concentration Cg the combustion rate is purely dependent on the chemical mechanism of the reaction. The rate of combustion per unit external surface can be expressed by:-

$k_{exp} = k_s . Cg^n . S_s$

k_s = reaction rate constant per unit B.E.T. surface
Cg = concentration of oxidants in the gas
S = B.E.T. surface of the sample
n = order of reaction
s = external surface of the sample
k_{exp} = rate per unit external surface

The chemical rate constant is related to the temperature by the Arrhenius equation:-

$$k_s = k_{s_0} e^{-E/RT}$$

The object of kinetic measurements is to study the order of the reaction (exponent n), and to determine the frequency factor k_{s_0} and the activation energy E. These values depend on the gaseous reactant, and the quality of the graphite (purity and structure).

2.1.2 *In-pore Diffusion*

At higher temperatures there is a concentration gradient in the porous material.

In this zone the reaction rate per unit area of external surface proceeds with an apparent activation energy of half the true value. A mathematical model of a porous material indicates that, in the in-pore diffusion controlled zone, the reaction rate is given, for a first order chemical reaction by:- [3]

$$k_{exp} = \sqrt{\frac{k_{s_0} Deff. 0. 2}{r}} \qquad (10)$$

0 = porosity of the sample
$Deff$ = effective diffusivity of the impurities in the pores
$\bar{r}$ = the mean pore radius

It can be seen from this equation that $k_{exp} \div e^{-E/2RT}$ which gives an activation energy of half that of the chemical rate.

It can also be seen that in this zone the rate is dependent on the texture of the graphite (0, $\bar{r}$, $Deff$, etc).

2.1.3 *Diffusion in the Gas Phase*

At higher temperature when the chemical reaction rate is very high, the rate determining step becomes the diffusion of oxidising impurities in the boundary layer.

In this zone the reaction rate is expected to be independent of the temperature, but in general a small activation energy is measured.

It is also interesting to note that in this high temperature region the reaction is neither dependent on the type of graphite used nor on the reacting gas. The reaction with O_2 and H_2O can be similar the rate of transfer of impurities being the only barrier.

Ultimately, at very high temperatures the rate of reaction can be expressed as the rate of mass transfer of reactants through the boundary layer.

This can be expressed as follows for a first order reaction:-

$k_s\, s.\, C_w = k_c\,(C_g - C_w).\ s$ (1)

k_s = chemical reaction rate constant cm/s

s = geometrical surface area cm^2

C_g = concentration of impurities in the main gas stream $mole/cm^3$

k_c = rate of mass transfer cm/sec

C_w = concentration of impurities on the wall of the reacting graphite $mole/cm^3$

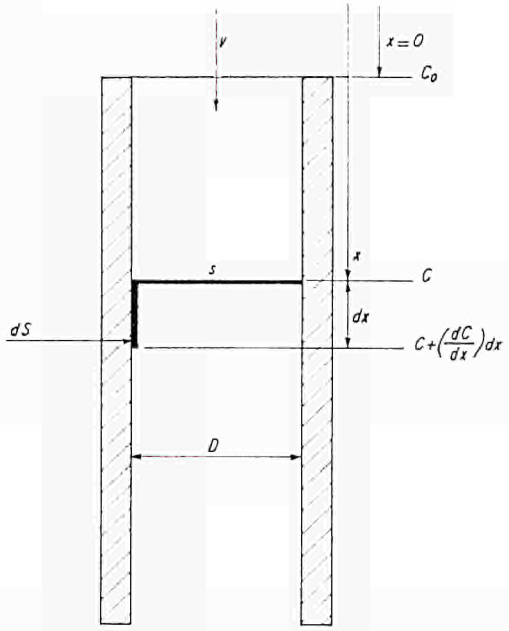

Fig. 3. Cylindrical channel with an axial flow.

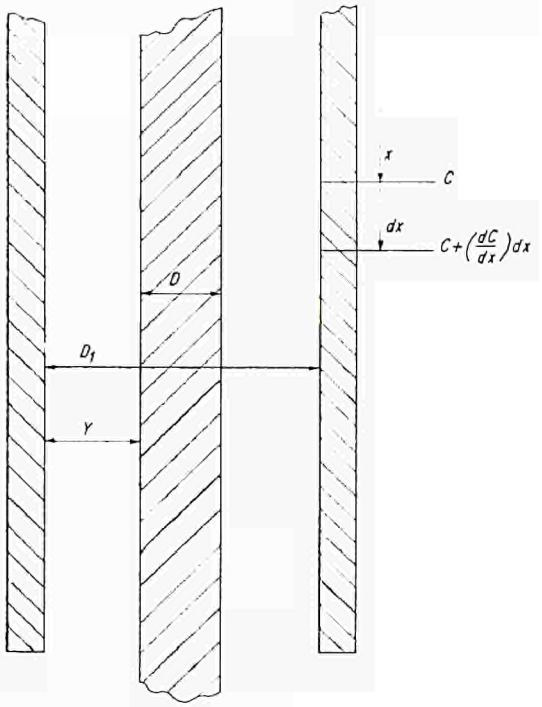

Fig. 4. Annular channel.

The concentration at the surface can be calculated from equation (1)

$$C_w = \frac{k_c}{k_s + k_c}\, C_g$$

The speed of reaction is then

$$\text{rate} = k_s \cdot \frac{(k_c)}{(k_s + k_c)}\ C_g\, s$$

It can easily be seen that

if $kc >> ks$ then

the rate $= k_s\, C_g\, s$, as for a normal chemical reaction.

if $ks >> kc$

rate $= k_c\, C_g\, s$, the reaction rate is only dependent on the rate of mass transfer.

Calculation of k_c

for a laminer flow one can write:-

rate $= C_g.\, D/\delta.\, s$ $\qquad kc = D/\delta$

D – is the Diffusion Coefficient

δ – is the thickness of the boundary layer.

For a turbulant flow the following equation based on Re analogy gives the kc

$$\frac{kc\ \ d}{D} = 0.023\ Re^{0.83}\ Sc^{0.44} \qquad (4)$$

Re = Reynolds Number

Sc = Schmidt Number

$$= \frac{\mu}{\varrho\ \ D} = \frac{\text{Kinetic Viscosity}}{\text{Diffusion coef.}}$$

Fig. 2 summarises some calculations of

(D for 1 and 20 atm
(kc for 1 and 20 atm and Re – 2,000 / 15,000
(Sc) of CO_2 in He

The chemical reaction rate corresponding to the specified material for Dragon is also known (See fig. 6 line (2) of D.P.R. 102).

Using this data it can be seen that with the surface temperature of 1,300°C, $Re = 15{,}000$, $P = 20$ atm and He at 750° C:

$$C_w = \frac{25.4}{25.4 + 8.1}\ .\ C_g \qquad C_w = 0.758\ C_g$$

Thus the concentration gradient in the boundary layer is detectable but negligeable under these conditions.

At higher temperatures and with more reactive graphite and lower Re this would not be the case.

For instance, it can be seen that with a gas flow at 600°C 20 atmosphere and $Re = 2000$ with the specified graphite at 1300° C, $C_w = 0.2\ C_g$. If the graphite used is ten times more reactive then $C_w = 0.024\ C_g$. This calculation indicates that mass transfer process is not negligeable in the H.T.G.R.

2.1.4 *In-pile Radiation Effect on Graphite Oxidation*

The intense radiation present in a nuclear reactor may lead to chemical reaction which would not otherwise occur. The types radiation which can effect the reactivity of graphite with gaseous reactants are principally gamma rays and fast neutrons.

Mass transport can be affected by in-pile radiation either by changing the rate of gasification of graphite or changing the rate of deposition of carbon.

The rate of gasification can be altered by creating active sites on the graphite surface or by creating active gaseous species.

2.1.4.1 *Activation of the reaction rate by creating active sites on the graphite surface*. The radiation of graphite with fast neutrons will give rise to localised defects:
Atomic Displacement: The radiation of graphite by high energy fast neutrons results in displacement of atoms in the lattice. The imperfections created in the lattice such as interstitial, lattice vacancies, or cluster of both and dislocation which act as active sites for the gasification reactions [5].
Thermal Spikes: A fast neutron will dissipate its energy in a very small volume of graphite. This region includes 5000 to 10,000 atoms and the localised T may rise by (700° C to 1200°C) for a period of $10^{-1}{}_0$ sec. The very rapid cooling resulting from the dissipation of heat in the surrounding material results in freezing of the disturbed lattice, since there is not sufficient time for all the atoms to be relocated in their equilibrium position. This disturbed lattice can act as an active site for the gasification reactions [6].
Catalytic Impurities: The basis of another explanation of increase in carbon gasification under radiation could be the transmutation of impurities present in the graphite into highly catalytic impurities. This explanation although possible has not been confirmed.

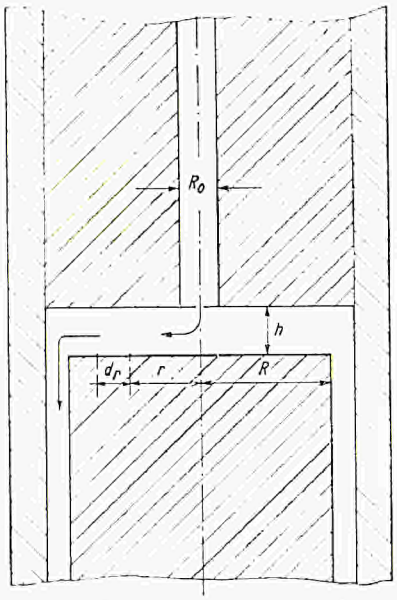

Fig. 5. Cylindrical channel with radial flow.

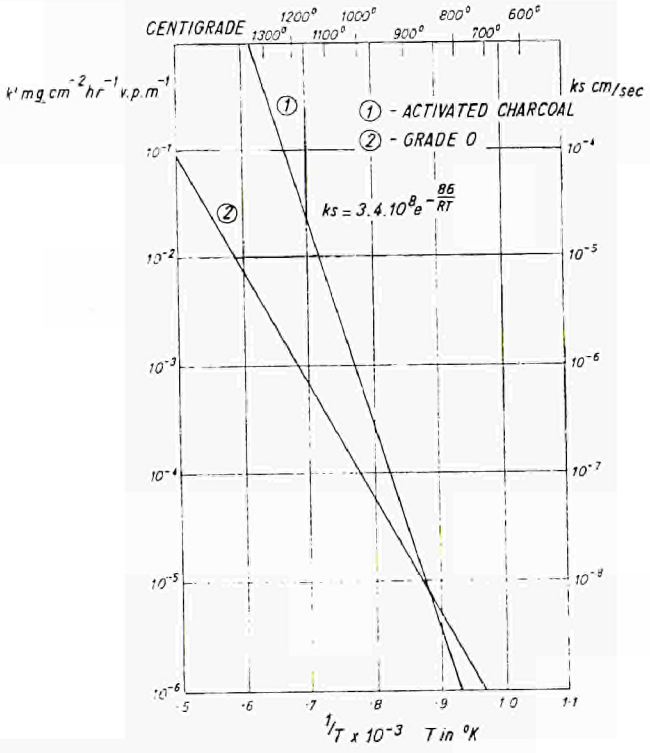

Fig. 6. Arrhenius plot of k (P.G.A.) and k_s (activated charcoal).

2.1.4.2 *Creation of Active Gaseous Particles in the Coolant*
It is generally accepted 'in the British Reactor School' that the enhanced increase in the reaction rate of (CO_2, H_2, O_2) with graphite is principally due to the creation of active gaseous species. This was an unexpected result because it was known that the major radiation energy absorption would occur in the graphite and not in the gas, but the experiments performed have shown that the accelerating effect of the reaction is mainly caused by the fraction of energy absorbed in the gaseous phase. Radiation produces new reactants by passing through intermediate species like atomic particles, ionised or excited molecules.

The rate of formation of new particles is a function of the energy absorbed in the gas. The degree of energy absorption depends on
The Reactor flux: its intensity in gamma and fast neutron distribution
G value: which is known approximately for pure gases like CO_2, and CO, but this may be affected by the presence of a carrier gas.

The mass of gas: submitted to radiation is also influencing the formation of new compounds. The effect of pressure is directly connected to the influence on the mass radiation.

The life time of the activated species is variable, consequently the steady state concentration of these species will be dependent on –
- Decay time of species
- Velocity of the gas
- Geometry of the system

An extrapolation from an in-pile test to a reactor system with different –
- Gas to graphite ratio
- Geometrical arrangement
- Velocity distribution
- Mass transfer rates, etc.

is difficult.

Temperature has no marked effect on the radiation induced reactions.

2.2 *Carbon Deposition*
As indicated in the definition of carbon transport the overall carbon transport process is due to reversible reactions. The most important reaction to be considered is the reverse of reactions (1) and (4) for C deposition.

Carbon deposition is catalysed by metallic surfaces such as *Fe* and *Ni*. The catalysis is enhanced by trace amounts of H_2. The reaction is strongly temperature dependent and reaches its maximum around 500° C to 600° C.

It is obvious that if back deposition was to be inhibited the balance of concentration of the impurities in a leak tight system would be displaced and the graphite corrosion would stop by lack of oxidising impurities.

The reaction can be inhibited by surface treatment such as cementation of the surface phosphatation.

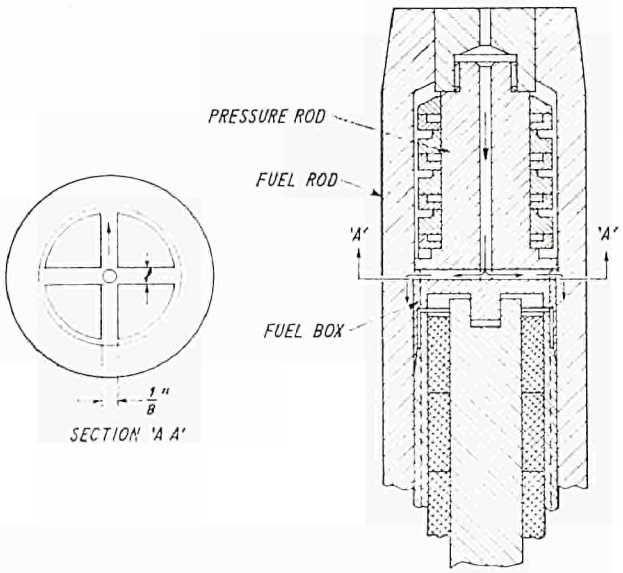

Fig. 7. Dragon purge flow inlet.

In the literature it is also reported that gaseous inhibitants such as H_2 S and SO_2 can be used.

2.3 *Clean-up Rate and Inleakage*

The balance of impurities present in the reactor will depend on the sources and sink of impurities.

The sources of impurities are:

The degassing of the components:

This sources, although not insignificant, due to the large amount of graphite and steel, is only temporary. It has to be considered at the start-up of the reactor.

The in-leakage rate:

Introduces impurities continuously from outside and therefore is more significant in time. In the Dragon reactor this source of impurity is unlikely because the steam in the heat exchangers is at a lower pressure than the primary circuit.

However, for a power reactor, the problem will be completely different and a figure of 5-lb/day steam inleakage is estimated for a 1000 MW reactor.

The Sink for Impurities is the Purification Plant

The gas purification rate of the primary circuit helium will also effect the level of impurity present in the system.

This factor cannot be enlarged at will, for economical reasons.

3. The Corrosion of Graphite in Dragon and the Depletion of Reactants

In a helium stream containing CO_2, flowing over a graphite surface at high temperature, there is a depletion of the oxidant concomitant to the corrosion of the graphite surfaces. The depletion depends on corrosion rates, the geometry of the system, and the flow rate.

Equations for various geometrical arrangements of the reacting graphite are established and calculations made for depletion rates in the purge and in the main flow assuming that the graphite has a reactivity similar to that of Grade *O*. The depletion rate calculation takes its full significance in the purge flow. It can be seen that a 5 vpm impurity level in the purge flow corresponds to $\sim$ 15 g graphite removed from each fuel rod for a three years of reactor operation.

Unfortunately it is incorrect to assume that the corrosion would be uniformly spread over the ten fuel boxes contained in a fuel rod. In actual fact, the reaction may be confined to the first centimeter of the first fuel box, causing very deep corrosion and possibly penetration. Apart from in this region, the corrosion will be negligible due to the depletion of the oxidants.

The distribution of corrosion and the rate of depletion of oxidants, based on the available temperature distribution curves [9] are considered below.

3.1 *Establishment of the Equations*

3.1.1

Consider the channel represented in Figure 3, in which we have:

C the CO_2 concentration at the distance x mole/cm^3

Table 1. Data for k/Q applicable to the purge flow.

1	2	3	4	5	6	7	8	9	10
k' mg cm^{-2} h^{-1} vpm^{-1}	k^* mg cm^{-2} h^{-1} vpm^{-1} at 20 atm.	k cm./s	k/Q	$\pi D\ k/Q$	$\pi D/Q\,(k_1+k)$	$x_{0.5}$ (cm.)	$x_{0.01}$ (cm.)	T (°C)	T (°K)
$3{\cdot}2 \times 10^{-3}$	$5{\cdot}42 \times 10^{-2}$	8·10	·166	2·317	3·256	·2128	1·416	1300	1573
$2{\cdot}0 \times 10^{-3}$	$3{\cdot}39 \times 10^{-2}$	4·60	·104	1·451	1·930	·3591	2·383	1250	1523
$1{\cdot}3 \times 10^{-3}$	$2{\cdot}20 \times 10^{-2}$	2·62	·0673	·939	1·185	·5848	3·890	1200	1473
$6{\cdot}6 \times 10^{-4}$	$1{\cdot}12 \times 10^{-2}$	1·52	·0343	·479	·5948	1·1651	7·751	1150	1423
$3{\cdot}4 \times 10^{-4}$	$5{\cdot}76 \times 10^{-3}$	·752	·0176	·2456	·3183	2·1772	14·483	1100	1373
$1{\cdot}6 \times 10^{-4}$	$2{\cdot}71 \times 10^{-3}$	·339	·00830	·1158	—	—	—	1050	1323
$1{\cdot}0 \times 10^{-4}$	$1{\cdot}70 \times 10^{-3}$	·206	·00521	·0727	·0858	8·0770	53·613	1000	1273
$1{\cdot}8 \times 10^{-5}$	$3{\cdot}06 \times 10^{-4}$	·0363	·000937	·0131	·0149	46·5	310·00	900	1173
$2{\cdot}5 \times 10^{-6}$	$4{\cdot}25 \times 10^{-5}$	·0043	·00013	·0018	—	—	—	800	1073
	(1) x 16·95		(2) x 3·062	(4) x 13·955	(5) + (5')	·693 ÷ (6)	4·61 ÷ (6)		

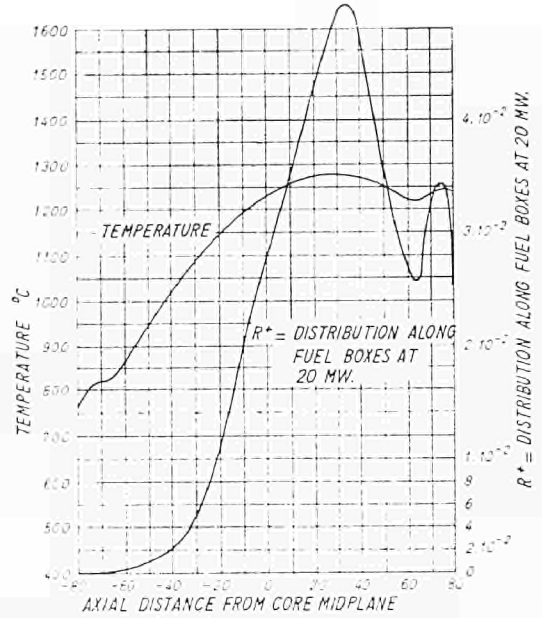

Fig. 8. Axial temperature k^* distribution along fuel boxes at 20 MW.

$C + \frac{\partial C}{\partial z} . dz$ the CO_2 concentration at the distance $z + dz$ mole/cm³

C_o	the CO_2 concentration at the distance $z = o$ mole/cm³	
v	the velocity of the gas	cm/s
V	the volume of the reactor	cm³
k	the reaction rate per unit external area of graphite	cm/s
Q	the volumetric flow of carrier gas	cm³/s
s	cross section perpendicular to the flow	cm²
dS	reacting surface along the dz distance	cm²
Pe	perimeter	cm

If the mass balance of reactant between section z and section $z + dz$ is considered; we equate the rate of variation of concentration to the rate of reaction with the graphite.

The number of mole CO_2 reacting between z and $z + dz$ for a gas circulating at a velocity v is:
$k . dS . dt . C$ with $dt = dz/v$

The resultant concentration change is given by:

$$dC = \frac{k . dS . dt . C}{dV}$$

Then

$$\frac{\partial C}{\partial z} . dz = - \frac{k . dS . dt . C}{dV}$$

$$\frac{\partial C}{\partial z} . dz = - \frac{k . d S. dz . C}{dV \quad V}$$

$$\frac{\partial C}{C} = - \frac{k . dS . dz}{dV . v} = - \frac{k . Pe . dz}{s . v} = - \frac{k . Pe . dz}{Q}$$

If the temperature is constant along the channel then k and Q are constant and:

$$C = C_o \, e^{- \frac{k \, Pe \, z}{Q}}$$

If the temperature varies along the channel, k and Q varies as a function of z

The equation to consider is then:

$$\log_e \frac{C}{C_o} = - \int_0^z \frac{k(z) \; Pe \; dz}{Q \; (z)}$$

3.1.2

For a cylindrical graphite tube with a constant axial temperature and with internal flow, the following equation can be written:

$$C = C_o \, e^{- \frac{k \, . \pi D \, . \, z}{Q}} \tag{10}$$

3.1.3

For a flow in an annulus between a cylindrical rod and a cylindrical tube, as shown in Figure 4, also with axial constant temperature, it can be easily seen that if the walls are reacting with the same k as the central rod.

$$C = C_o \, e^{- \frac{k\pi \, (D \, + \, D_1)}{Q} \, . \, z} \tag{11}$$

If y is small, or $D \simeq D_1$

$$C = C_o \, e^{- \frac{2k \, \pi D}{Q} \, . \, z} \tag{12}$$

If the reaction rate k_1 of the vessel surface is different from the k of the central rod, we can write:

$$C = C_o \, e^{- \left[\frac{k_1 \, \pi \, D_1}{Q} + \frac{k \, \pi \, D}{Q} \right] z} = C_o \, e^{- \frac{\pi (k_1 D_1 + kD)}{Q} z} \tag{13}$$

3.1.4

For the flow in the cylindrical space above a reacting top cover at constant temperature (Figure 5) assuming a central feeding of the reactant, we know that:

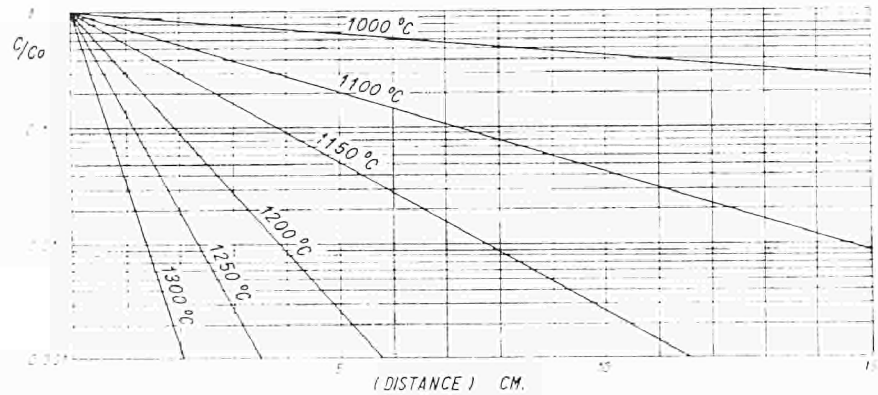

Fig. 9. Depletion rate along fuel boxes at various temperatures.

$$\frac{\partial C}{\partial r} \cdot dr = -\frac{k \cdot dS \cdot dt \cdot C}{dV}$$

$$ds = 2\pi r\, d r$$

$$dV = 2\pi r\, dr\, h$$

$$dt = \frac{dV}{Q} = \frac{2\pi r\, dr\, h}{Q}$$

$$\frac{\partial C}{\partial r} = -\frac{k\, 2\pi r\, C}{Q}$$

$$\frac{\partial C}{C} = -\frac{k\, 2\pi r\, dr}{Q}$$

Assuming $R_o = O$ and integrating:

$$C = C_o\, e^{-\frac{k\pi r^2}{Q}} \qquad (14)$$

Equation 14 gives the concentration of impurities at the distance r from the centre.

3.1.5

In the case of flow in a cylindrical space above a top cover, assuming that the cylindrical space is filled with a porous material reacting with the reactant centrally fed, we must use k_s rate per unit area B.E.T. for the internal surface.

Up to now we have used a k value which refers to the external surface of the reacting body.

The volume of porous material between r and $r + dr$ is $2\pi r\, dr\, h$, consequently:

$dS = 2\pi r\, dr\, h\, \varrho\, Sg$

Sg = the B.E.T. surface per gramme porous material cm^2/g

ϱ = the density g/cm^3

ϱSg = the surface B.E.T. per unit volume cm^2/cm^3

$$dt = \frac{Vg\, \varrho\, 2\pi r\, dr\, h}{Q} = \frac{02\pi r\, dr\, h}{Q}$$

Vg = the pore volume per gramme of the porous material

0 = the porosity of the material.

$dV = 2\pi r\, dr\, h\, 0$ = free volume.

Consequently:

$$\frac{\partial C}{\partial r} \cdot dr = -\frac{k_s\, 2\pi r\, dr\, h\, \varrho\, Sg\, C}{Q}$$

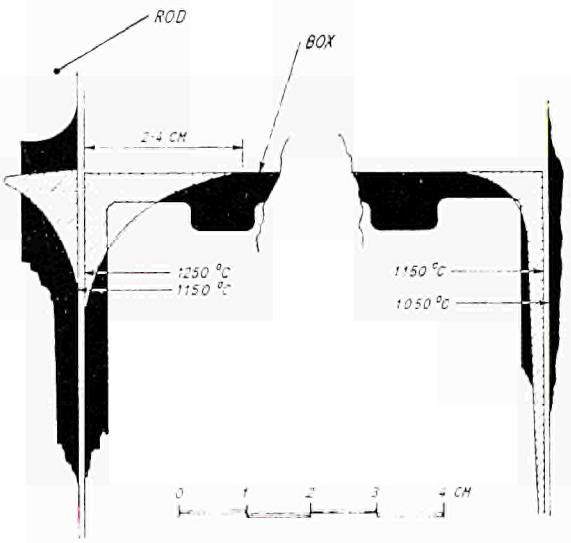

Fig. 10. Typical fuel box corrosion (5 VPM CO_2 20 atmosphere) in 3 years.

If R_o is assumed very small compared to R

$$C = Cg\, e^{-\frac{k_s \pi r^2 h \varrho\, Sg}{Q}} \qquad (15)$$

$$C = C_o\, e^{-\frac{k_v \pi r^2 h}{Q}} \qquad (16)$$

where $k_v = k_s\, \varrho\, Sg$ the reaction rate per unit volume is expressed in $1/s$.

3.2 *Experimental corrosion rates*

As already established the k value is an important factor in the depletion rate calculation. This value depends on the graphite quality and temperature. We use in our calculation the k value obtained experimentally with Pile Grade A in reaction with CO_2.

Figure 6 line (2) shows the corrosion rates of P.G.A. in an Arrhenius plot log k' versus $1/T$ $(1/°K)$. k is expressed in mg. $cm^{-2}\, hr^{-1}\, vpm^{-1}$. This k' value is related to the geometrical surface area of the reacting body with the CO_2.

The corrosion rate fits in with the equation $k' = Ae^{-E/RT}$ where the activation energy E is approximately 45 *kcal/mole*.

It must be noted that this corrosion rate is obtained with 200 *vpm* CO_2 in helium in presence of a high concentration of CO, CO/CO_2 ratio being 10/1.

Figure 4 line (1) shows rate constant k_s in *cm/s* for an activated charcoal, the characteristics of which are as follows:

Ash content 0.14–0.17
Density ϱ 0.51
Porosity 85%
Specific Surface Area 700 m^2/g = 7.10^6 cm^2/g.

The rate constant has been obtained experimentally in tests where the diffusion controlling steps are eliminated [1]. Thus, the activation energy of 86 *kcal/mole* is obtained.

$$k_s = 3.4\ 10^8\ e^{-\frac{86}{RT}}$$

In the case of a porous pellet with a forced high flow through it, the use of this reaction rate constant is justified.

3.3 *Depletion rate along the slots of the pressure rod*

With the present fuel design element the purge gas reaches the top of the first fuel box through a central hole in a pressure rod resting on the lid of the top fuel box. The gas flows towards the periphery of the fuel box along four channels forming a cross channel (Figure 7).

The purge flow in the reactor is 5.10^3 cm^3/s at 20 atm and 350°C. This purge flow in the reactor is divided between the 259 fuel rods. Table 1 gives the relevant data k/Q for the purge flow as calculated in Annex 1.

As indicated in Figure 8 the top cover of the fuel boxes range from 1000° C to 1150°C depending on the radial location of the fuel element in the reactor. A typical k*distribution along the boxes is also given in Figure 8.

The depletion of the reactant along the length of the four channels has been calculated assuming that only the face in contact with the lid of the box reacts. It is also assumed that the top cover is at constant temperature, and typical examples are calculated for 1000°C and 1100°C.

3.3.1 *Top Box at* 1000° C.

$$\frac{C}{C_o} = e^{-\frac{k\, l}{Q/4} R}$$

$$4\frac{k}{Q} = .00521 \times 4$$

$$\frac{C}{C_o} = e^{-0.02084\ 1\ R}$$

$l = 0.125'' = 0.317$ cm.

$R = \frac{1.749''}{2} = 2.221$ cm.

The term $Q/4$ comes from the fact that the purge flow is divided into four legs.

$C = C_o\, 0.985$

3.3.2 *Top Box at* 1100° C.

$\frac{C}{C_o} = e^{-0.0495}$

$C = C_o \times 0.95$

It can then be seen that the depletion along the top cover is not very important. Moreover, by this arrangement if 5 *vpm* CO_2 is admitted in the purge flow four grooves of 4.4 mm maximum depth will be burned into the top lid at 1100° C after a 3 year operation.

3.4 *Depletion rate along fuel boxes*

As shown the depletion rate along the top cover is negligible. It may then be assumed that in the annulus between the fuel rod and the fuel boxes, a concentration reactant of C_o is established.

By inserting in equation (4) the dimension of the fuel box and characteristics of the purge flow, and moreover assuming a uniform reaction rate along a short length of the box, the distance is calculated at which the concentration is decreased by a factor 2 and by a factor 100. The results are tabulated in Table 1.

It is assumed that the inner wall of the fuel tube has a temperature, 100° C lower than the temperature of the adjacent fuel box. Let us take as an example the case of a top box at 1250° C and the adjacent inner fuel rod at 1150° C.

$\frac{\pi D}{Q}(k_1 + k) = 1.930$

$C = C_o\, e^{-1.930\, x}$

$x_{0.5} \simeq .35$ cm

$x_{0.01} \simeq 2.3$ cm

Consequently the CO_2 level will be reduced to 50% of its initial value after .35 cm and to 1% of its value after 2.3 cm if the gas is in contact with a fuel box at 1250° C and a fuel rod surface at 1150° C. This can also be seen by considering Figure 9.

The analysis given above is inaccurate due to the fact that it assumes a constant temperature along the fuel box.

A more accurate calculation can be obtained by taking into account the fluctuation of $(k_1 + k)$ over the length of the fuel boxes. Then the formula giving C can be written as follows:

$$\log_e \frac{C}{C_o} = -\pi D \int_{x=-80}^{x=80} \frac{(k_1 + k)\, dx}{Q}$$

The integral value may be obtained by graphical integration along the length. Figure 8 shows a typical temperature distribution [9] and the corresponding k^* value along the box. Because the depletion occurs along a very short length with an approximately uniform temperature gradient the expression is not integrated.

Figure 10 shows schematically the corrosion to be expected along a fuel box. It has been assumed that C_o was 5 *vpm*. The right hand side of the figure shows what might be expected with a fuel box at 1150° C and the left hand side shows what might occur with a box at 1250 °C.

From the radial temperature distribution in the core at 20 MW. Figure 11, it can be seen that approximately 30% of the fuel rods are in the hot zone 1250° C [9].

The real corrosion process will be more complex than shown in Figure 10: because as soon as the corrosion proceeds the annular gap between the box and the fuel rod increases. The temperature of the box will then increase and that of the fuel rod decrease. Moreover the residence time of the gas in the enlarged gap will also be different.

3.5 *Effect of a porous plug inserted between the pressure rod and the first fuel box*

It has been suggested that a graphite porous pellet inserted on the top of the first box might act as a getter for oxidant impurities. In the calculation to assess its efficiency the thickness of this porous plug is assumed to be 1 cm. A thicker porous plug may not be efficient due to the temperature drop in that part of fuel element. Equation 15 or 16 gives the depletion rate.

The following assumptions for the porous plug have been made. It has the *Sg* and ϱ and k_s of activated charcoal.

We consider three possible temperatures of a porous plug on top of a fuel box. 900° C for the coldest channel, 1000° C and 1100° C for the hottest channel in the reactor.

3.5.1 900° C.

$k_s = 3.5\ 10^{-8}$ cm/s (Taken from Figure 4)

$$\frac{C}{C_o} = e^{-\frac{3.5\ 10^{-8} \times 3.14 \times (2.22)^2 \times 1 \times 0.51 \times 7.10^6}{36.3}}$$

$= e^{-0.0526}$

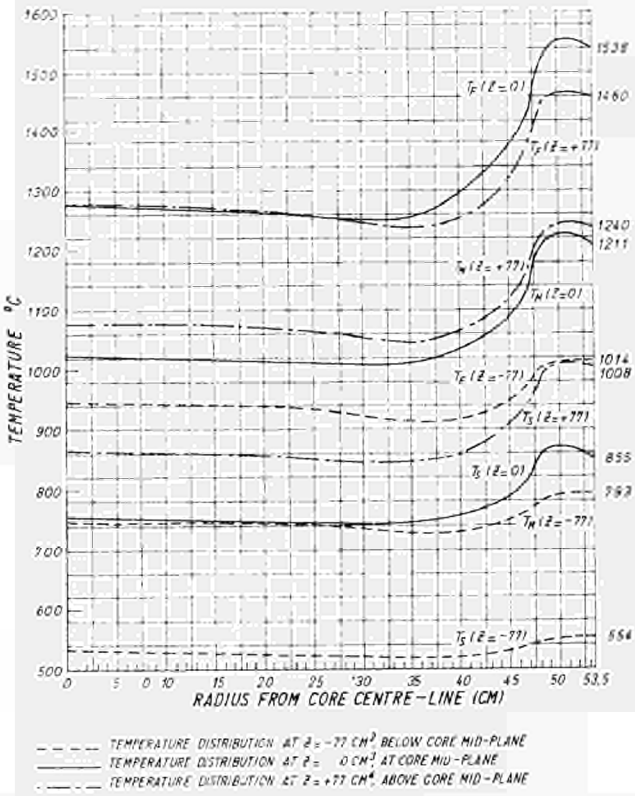

Fig. 11. Radial temperature distribution in the core at 20 MW.
T_S = Fuel rod surface temperature
T_M = Average moderator temperature.
T_F = Maximum fuel temperature.

Which gives a very low porous pellet efficiency.

3.5.2 1000° C.

$$\frac{C}{C_o} = e^{-0.995}$$

3.5.3 1100° C.

$k_s = 7.10^{-6}$ (Taken from Figure 4).

$$\frac{C}{C_o} = e^{-8.96}$$

It is apparent then that the efficiency of a porous plug as a getter is very temperature dependent. Its efficiency is complete for a 1100° C porous plug but negligible at 900° C and not sufficient at 1000° C.

It is problematic to maintain a porous material at a temperature of 1100° C over a thickness of 1 cm on the lid of the top box. The use of a more reactive material can probably decrease the required operating temperature.

3.6 *Corrosion along the fuel channel*

The temperature distribution along the fuel channel at radius $R = 50$ cm of the reactor core, is given in Figure 12 (1). The corrosion rate distribution corresponding to this temperature distribution is also indicated in the Figure 12 (2).

The depletion rate along the rod will be given by:

$$\frac{\partial C}{C} = -\frac{k_{(\kappa)}\, Pe\, d\varkappa}{Q_{(\kappa)}}$$

k and Q are variable with ($\varkappa$). $k^*_{(\kappa)}$ function of $\varkappa$ is given by curve (2) of Figure 12.

$$\log_e \frac{C}{C_o} = -Pe \int_{\alpha=-80}^{\alpha=80} \frac{k_{(\kappa)}\, d\varkappa}{Q_{(\kappa)}}$$

If $k^*_{(\kappa)}$ is expressed in mg. cm^{-2} hr^{-1} vpm^{-1} and $k_{(\kappa)}$ in cm/s we know that a relation of the type $k_{(\kappa)} = k^*_{(\kappa)}\, T_{(\kappa)}\, gas\, C_1$ exists between $k_{(\kappa)}$ and $k^*_{(\kappa)}$

$$\left(C_1 = \frac{R \times 10^6}{P \times 12.000 \times 3.600} = 0.0949\right)$$

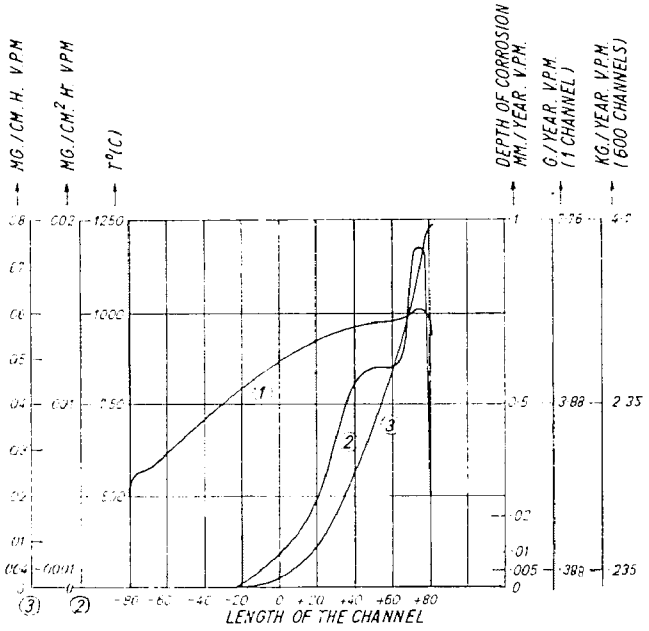

Fig. 12. Temperature and corrosion distribution along a fuel rod.

Moreover $Q_{(\kappa)} = \frac{Q_o}{T_o} T_{(\kappa)}\, gas$

Consequently:

$$\frac{k_{(\kappa)}}{Q_{(\alpha)}} = \frac{k^*_{(\kappa)}\, T_{(\kappa)}\, gas\, C_1}{\frac{Q_o}{T_o} T_{(\kappa)}\, \text{gas}}$$

$$= \frac{k^*_{(\kappa)}\, C_1}{Q_o} T_o$$

$$\int_{-80}^{80} \frac{k_{(\kappa)}}{Q_{(\alpha)}} d\varkappa = \frac{T_o}{Q_o} \int_{-80}^{80} k^*_{(\kappa)}\, C_1\, d\varkappa$$

Then:

$$\log_e \frac{C}{C_o} = \frac{T_o}{Q_o} Pe \int_{-80}^{80} k^*_{(\kappa)}\, C_1\, d\varkappa$$

The integral is obtained by a graphical integration.

Curve (3) Figure 12 gives:

$$\int_{-80}^{80} k^*_{(\kappa)}\, d\varkappa \; mg.\, hr^{-1}\, cm^{-2}\, vpm^{-1}$$

$$Pe \int_{-80}^{80} k^*_{(\kappa)}\, d\varkappa \; mg.\, hr^{-1}\, vpm^{-1}$$

is obtained per channel, taking into account that Pe the perimeter of the trefoil channel is 11.06 cm.

The Q_o value per coolant passage can be obtained approximately by multiplying the cross sectional area of the passage 2.27 cm^2 by the mean value of the gas velocity at $T_o = 350°$ C.

$Q_o = 2.27 \times 5012 = 1.163 \times 10^4$ cm^3/s.

At the end of the hottest channel:

$$C = C\, e^{-\frac{623 \times 0.079 \times 11.06 \times 0.0949}{1.163 \times 10^4}}$$

$$C = C_o\, e^{-0.00433}$$

$$C \simeq 0.9956\, C_o$$

It can thus be seen that the depletion rate along the channel is negligible. After consideration of Figure 12, it may be seen that curve (2) also represents the depth of corrosion mm/year vpm.

Curve (3) also gives the total amount of graphite removed from the core per vpm.

4. Conclusions

From the previous calculations, an approximate picture can be obtained of the corrosion distribution in the reactor along the hot graphite surfaces which come into contact with flowing gas.

To the calculations have been performed with the following assumptions and simplifications with made:

4.1

The reactivity k used for the graphite is an experimental reactivity obtained on P.G.A. graphite. The graphite to be used in the reactor will probably have a different reactivity.

4.1.2

The k quoted has been obtained at atmospheric pressure, and extrapolated to 20 atm.

4.1.3

The reaction rate k may be limited at high temperature by gas phase diffusion in the low Re region.

4.1.4
The effect of radiation on the k has not been taken into account. Moreover in our discussion we neglect the possible C_o — C radiation induced reaction.

4.1.5
Mechanical erosion has also been neglected.

4.1.6
The calculations assumed a steady temperature distribution along one rod. However, the temperature distribution in the reactor varies from rod to rod, and for a given rod it varies with time.

Reactor operation at lower temperature may also affect the temperature level and distribution. Moreover recent calculations tend to indicate that the temperature of the fuel will be higher than those used in the calculations. The temperatures used in the calculations were obtained assuming 18.25 MW generated in the fuel rod and 1.75 MW in the reflector. The latest figures are 19.4 MW in the core and 0.6 MW in the reflector. [9].

4.1.7
It was assumed that the graphite attack would be uniform, although some experimental evidence indicates that above 1100° C pitting occurs.

4.1.8
Reactions have been assumed to be of the first order. Bearing in mind these restrictions, we may conclude:

4.2.1 *For the Fuel Boxes*
4.2.1.1 The fuel element in its actual design might suffer from a cruciform corrosion on the lid of the first box. The depth of this corrosion will depend on the temperature of each fuel element and on the concentration of impurities in the purge flow.

As an example, a top cover at 1100° C would be corroded to a depth of 4.4 mm after 3 years in a stream containing 5 vpm CO_2.

4.2.1.2 The depletion rate of impurities along the lid of the top fuel box is not sufficient to avoid a further corrosion along the side of the first fuel box.

For the hottest boxes at approximately 1300° C the depth of denetration, a function of the CO_2 concentration, decreases exponentially from the top and after 1.416 cm the rate of reaction is decreased by a factor of 100.

Using the reactivity of P.G.A. and assuming a CO_2 content of 5 vpm it can be seen that where the corrosion starts 4 cm would be removed from the thickness of the box per three years, and 1.65 cm from the thickness of the adjacent fuel rod which is supposedly at 1200° C. This means that the useful life of the fuel element might be very much shorter than 3 years because the thickness of the fuel rod is less than 4 mm.

For a box at 1100° C the damage is spread over a longer distance approximately 15 cm, but the deepest attack will be approximately 4 5 mm per 3 years.

Consequently favoured by the steep temperature gradient existing at the top of the core, the top fuel box and the adjacent fuel rod can be attacked locally.

The real corrosion process will be more complex, as already stated, because during the process of corrosion the fuel box temperature will increase, while the fuel rod temperature decreases, and the residence time of impurities is also longer in an enlarged annular gap.

4.2.1.3 The installation of an active charcoal pellet will only be effective in removing the oxidising elements if it can be maintained at a high temperature (above 1000° C).

The use of a more reactive material can decrease the required operating temperature.

4.2.1.4 Another method of removing the impurities would be the use of a hot metal getter which can operate at lower temperature (600° C.). The advantage of a hot metal getter [10] would be to remove the CO as well, and so avoid any radiation induced between CO an C.

4.2.2 *For the Fuel Rod*
Due to the temperature distribution the maximum depth of corrosion will be localised at the top of the fuel rod. When this depth reaches the maximum admissible value of 0.5 mm the core will have lost 25 kg of graphite (41.5 g per channel).

There is only a negligible depletion of the reactant at each passage over the fuel rod. (0.5%).

5. Acknowledgements

The numerical and graphical computations performed by Mr. P. de Windt and Mr. M. I. Hawker.

6. References.

[1] D.P.Report 75
[2] P. Walker et Al; Advance in catalysis Vol
[3] Ahlborn Wheeler; Advance in catalysis Vol III
[4] Chemical Engineering Series
Trey bal Mass Transfer Operations
[5] G. R. Hennig et Al; Radiation effects on the oxidation rate of graphite P/1778.
[6] S. Gladstone; Principle of Nuclear Reaction Engineering
[7] P. S. Bourke, W. H. Denton; Carbon transport Problems in a High Temperature Gas Cooled Graphite Reactor A.E.R.E. – R 3916
[8] E. Wicke and H. H. Kopper; Röntgenstruktur und chemische reaktionsfähigkeit verschiedener Kohlenstoffproben. Journal de Chimie Physique. Tomme 50 No. 1.
[9] D. A. Hawkes; Dragon Data Sheets and Private Communication.
[10] D. Kinsey; Private Communication.

Annex

Calculation of the purge flow data

The experimental reaction rate column k' measured at 1.8 atm expressed in mg/cm² hr vpm is converted into the k^* column 2 expressed in mg/cm² hr vpm at 20 atm.

The k value expressed in cm/s column 3 is obtained by:

$$k = \frac{R \times T \times 10^6}{P \times 12.000 \times 3.600} \times k^* \text{ cm/s}$$

$$k = T \times 0.0949 \times k^*$$

The flow Q_o at 350° C and 20 atm is per fuel rod:

$$Q_o = \frac{5.10^3}{2.59} = 19.3 \text{ cm}^3/\text{s}$$

$$T_o = 350° \text{ C} = 623° \text{ K}$$

The $\frac{k}{Q}$ column 3 value is obtained:

$$\frac{k}{Q} = \frac{T \times 0.0949 \times k^* \times 623}{Q_0 \times T}$$

$$\frac{k}{Q} = 3.062\ k^*$$

The diameter of the fuel box is:

$D = 1.749'' = 4.442$ cm.

Column 4 is then calculated:

$$\frac{\pi Dk}{Q} = 13.955 \frac{k}{Q}$$

The column 6 is obtained by adding the $\pi Dk/Q$ of column 5 to the $\pi Dk_1/Q$ of the same column (5) taken at temperature 100° C and lower.

Column 7:

$$z_{0.5} = \frac{0.639}{\frac{\pi D}{Q}(k_1 + k)} \text{ cm}$$

Column 8:

$$z_{0.01} = \frac{4.61}{\frac{\pi D}{Q}(k_1 + k)} \text{ cm.}$$

Discussion

J. P. W. Houtman: Can one expect the radiation damage of graphite to have a big influence on the reaction rate with oxygen.

Answer b:

L. Valette: The only experimental evidence on the enhancement of the oxidation of graphite by neutron irradiation has been given by G.R. Hennig who has observed *out of pile* a higher reaction rate with a pre-irradiated graphite specimen. At temperatures above 600° C the increase in reaction rate disappears because of thermal annealing of the radiation damage.

H. de Bruijn: However, it may be that *inpile* neutron irradiation has an influence on graphite oxidation also above 600° C. We are dealing with a steady state of active sites determined by the competition of an annealing process of defects and of the creation of new defects. The new defects will be produced by the oxidation itself and by impact of fast neutrons with the graphite lattice. On the other hand, the fast neutrons may also facilitate the annealing process, therefore offhand one cannot predict whether there will be a negative or positive catalytic effect of irradiation if there is any.